

Do nucleons in abnormal-parity states contribute to deformation?

K. H. Bhatt

*Department of Physics and Astronomy, University of Mississippi, University, Mississippi 38677
and Joint Institute for Heavy-Ion Research, Holifield Heavy Ion Research Facility, Oak Ridge, Tennessee 37831*

C. W. Nestor, Jr. and S. Raman

Oak Ridge National Laboratory, Oak Ridge, Tennessee 37831

(Received 13 March 1992)

We consider intrinsic states of highly deformed nuclei in the framework of the universal Woods-Saxon model and show that valence nucleons in abnormal-parity high- j states contribute $\sim 20\%$ to the electric quadrupole moments of these nuclei. Similarly, we show that in the single-shell asymptotic Nilsson model this contribution is $\sim 25\%$ if reasonable effective charges are employed. We discuss, at some length, procedures used to arrive at reasonable effective charges. Both models reproduce the measured $B(E2; 0_1^+ \rightarrow 2_1^+)$ values in the rare-earth and actinide regions without the need for normalization constants. No support is found for the assumption made in the pseudo-SU(3) and the fermion dynamic symmetry models that valence nucleons in abnormal-parity high- j states do not contribute to deformation. This counterintuitive assumption leads to an underestimate of the $B(E2; 0_1^+ \rightarrow 2_1^+)$ values, which is compensated in these models by the use of appropriate normalization constants. Once the magnitudes are fixed, both models do correctly reproduce the $B(E2)$ trends.

PACS number(s): 21.60.Fw, 21.60.Cs

I. INTRODUCTION

A basic property of a nucleus is the probability of electric quadrupole ($E2$) transitions between its low-lying states. In even-even nuclei, the reduced $E2$ probability $B(E2; 0_1^+ \rightarrow 2_1^+)$ from the 0_1^+ ground state to the first-excited 2_1^+ state [1,2] is especially important, and for a deformed nucleus this probability [denoted here by $B(E2)\uparrow$] depends on the magnitude of the “intrinsic” quadrupole moment (quadrupole moment of the intrinsic state of the nucleus) and, hence, on deformation. In this paper we consider nuclear deformation as a given and do not enquire how it is generated by microscopic interactions.

In a shell-model framework, properties of low-lying states of nucleus are determined by valence nucleons moving in single-particle orbits within a major shell defined by the magic numbers. The contribution of the core to the intrinsic quadrupole moment (that is, the polarizing effect of interactions of a valence nucleon with core nucleons) is usually taken into account by associating an effective charge with a valence proton or neutron. On the other hand, in the case of “universal” models employing either a folded-Yukawa [3] or Woods-Saxon [4] potential, the intrinsic state is calculated by explicitly including all nucleons. Because these models calculate the total electric quadrupole moment of *all* protons and not just valence ones, it is not necessary to employ effective charges, as is done in a shell model.

Again, in a shell-model framework, the intrinsic quadrupole moment of a nucleus is determined by the mass quadrupole moment of valence nucleons and their effective charges. The magnitudes of the mass quadrupole moment can be different for different models with

the same single-particle valence space, but the effective charges that simulate the coherent quadrupole polarization of the core [5] should be the same for different models with the same core.

An interesting question is the relative contributions of nucleons in the so-called “normal-parity (n)” and “abnormal-parity (a)” single-particle states in a major shell to the magnitude of the intrinsic quadrupole moment. For protons (Z) or neutrons (N) in the 28–50, 50–82, 82–126, and 126–184 regions, the “abnormal-parity” single-particle states are the $1g_{9/2}$, $1h_{11/2}$, $1i_{13/2}$, and $1j_{15/2}$ states with high angular momenta (high- j) embedded within (or intruding into) the bunch of “normal-parity” states. This question is interesting for the following reason. From the simple Nilsson model [6] (with or without $2\hbar\omega$ mixing) to more complicated universal models, most models suggest that occupied abnormal-parity states play an important role in determining the magnitude of the quadrupole moment of the intrinsic state. Mean-field calculations [7,8] also arrive at the same conclusion.

By contrast, the pseudo-SU(3) model [9] as well as the fermion dynamical symmetry model [10] require, at least in their simpler versions, nucleons in an abnormal-parity high- j state to be coupled to a seniority-zero state even when remaining nucleons (in normal-parity states) of a particular valence shell are in a maximally deformed state. Thus nucleons in an abnormal-parity state do not contribute actively (via their quadrupole moments) to the magnitude of deformation while still contributing passively to its trend by influencing the sequence of occupation of normal-parity states. It is an aim of this paper to inquire how well this diminished role assigned to abnormal-parity states in these models is justified. This

question can be answered *only* if the same effective charges are employed *ab initio* for all models with the same core.

We have shown elsewhere [11,12] that a variety of schematic shell models can reproduce deformation trends in a satisfactory manner so long as the concepts of magic numbers and effective charges are integral parts of such models. With a “reasonable” choice of effective charges, agreement with the magnitude of deformation in each region can then be achieved through an overall normalization factor. If this factor is also reasonable (say, close to unity), it can be claimed that a particular model has greater validity, at least for this purpose, than if this factor were significantly different from unity. Therefore, in this paper, we wish to keep close track of this factor.

This paper is organized as follows. In Sec. II we recapitulate basic formulas relating measured $B(E2)\uparrow$ values to mass quadrupole moments of protons and neutrons and their effective charges. We discuss our choice of reasonable effective charges. We show that information obtained in the framework of the universal Woods-Saxon model (UWSM) concerning intrinsic mass quadrupole moments of protons and neutrons may be used to deduce an effective charge for valence neutrons. For a particular nucleus, the same model gives the fractional contributions of valence nucleons in abnormal-parity states to its total intrinsic mass and electric quadrupole moments. We also describe in this section the procedure followed to determine whether the Nilsson model or the pseudo-SU(3) model or, for that matter, any other shell model gives the correct magnitude of nuclear deformation.

The UWSM does have ten parameters defining the Woods-Saxon potential, and extensive computations are required to determine equilibrium deformations; however, good agreement with $B(E2)\uparrow$ data is achieved in all regions (see, for instance, Ref. [13] for data in the rare-earth and actinide regions) without effective charges and with an overall normalization factor *very close to unity*. Moreover, this model does not treat abnormal-parity states in any special way. In Sec. III we use this model and expressions given in Sec. II to calculate neutron effective charges and abnormal fractions of quadrupole moments for selected nuclei.

In Sec. IV, we consider the single-shell asymptotic Nilsson model (SSANM). We first show that this model gives the correct magnitude of mass quadrupole moments in the sense that measured $B(E2)\uparrow$ values are optimally reproduced with reasonable effective charges and an overall normalization factor *close to unity*. We then calculate abnormal fractions of the total intrinsic mass and electric quadrupole moments of selected nuclei using this model also.

Section V contains a description of the pseudo-SU(3) model (PSM), its basic assumptions, and its use in calculating intrinsic quadrupole moments. We show that the model assumption of seniority-zero coupling for nucleons in abnormal-parity states leads to an underestimate of the intrinsic quadrupole moment. To restore good agreement with measured $B(E2)\uparrow$ values, it is necessary to use a normalization factor that is appreciably *greater than unity*. The fermion dynamical symmetry model (FDSM)

treats nucleons in abnormal-parity states in a similar way, but the contexts in which SU(3) symmetry arises for normal-parity states are quite different in these two models. Therefore intercomparisons between them and between measured $B(E2)\uparrow$ values and predictions are also of interest. A summary appears in Sec. VI.

II. INTRINSIC $E2$ MOMENTS AND EFFECTIVE CHARGES

The $B(E2)\uparrow$ value of a deformed nucleus is given to a good approximation [14] in terms of the electric quadrupole moment Q_0 by

$$B(E2)\uparrow = (5/16\pi) |Q_0|^2 . \quad (1)$$

If the nucleus is described in terms of the UWSM, which includes explicitly core (c) as well as valence (v) nucleons, Q_0 is just the intrinsic quadrupole moment of all protons (π). Therefore

$$Q_0 = eQ_\pi = e[Q_\pi^c + Q_\pi^v] , \quad (2)$$

where e is the proton charge and Q_π the mass quadrupole moment of protons, which is split into a Q_π^c part for core protons and a Q_π^v part for valence ones. In this paper we count as valence nucleons those exceeding the adjacent magic number. The mass quadrupole moment of neutrons (ν) also has Q_ν^c and Q_ν^v parts which do not contribute, in the UWSM, to the electric quadrupole moment.

In a shell-model description, Q_0 is defined in terms of the mass quadrupole moment Q_π^v (Q_ν^v) and effective charges e_π (e_ν) of valence protons (neutrons) by

$$Q_0 = e_\pi Q_\pi^v + e_\nu Q_\nu^v . \quad (3)$$

Effective charges e_π (e_ν) may be written as

$$e_\pi = e(1 + \alpha_\pi) \quad \text{and} \quad e_\nu = e\alpha_\nu , \quad (4)$$

where α_π and α_ν take into account the effect of the quadrupole polarization of core protons by valence nucleons. Using self-consistency arguments, Bohr and Mottelson [15] have estimated, as a first approximation, that $\alpha_\pi = \alpha_\nu = Z/A$, but they have also suggested that α_ν should be somewhat greater than α_π because the interaction between a neutron and a proton is stronger than that between two protons (or neutrons). Therefore we rewrite Eqs. (4) as

$$e_\pi = e[1 + (Z/A)] \quad \text{and} \quad e_\nu = e(Z/A)\epsilon , \quad (5)$$

where the parameter ϵ , determining the neutron effective charge, can vary from 1 to 3.2. [When $\epsilon = 3.3$, e_ν exceeds e_π for ^{156}Er , ^{158}Yb , ^{164}Hf , ^{168}W , ^{172}Os , and ^{176}Pt for which measured $B(E2)\uparrow$ values are known and $e_\nu > e_\pi$ is unreasonable.] The average value of ϵ between these two extremes is 2.1. We consider $e_\pi = e[1 + (Z/A)]$ and $e_\nu = e(Z/A)2.1$ to be *reasonable* effective charges for heavy deformed nuclei.

What are some semiempirical e_π and e_ν values obtained in shell-model calculations for heavy spherical nuclei near closed shells? Byrne *et al.* [16] found that $e_\pi = 1.5e$ reproduced the measured quadrupole moment

of the 2849-keV 11^- state in ^{210}Po and of the 2641-keV, $\frac{29}{2}^+$ state in ^{211}At . In ^{212}Rn , Warburton and Brown [17] found that $e_\pi = 1.27e$ gave the best fit to $E2$ data. For neutrons the average of effective charges deduced by Yoshida and Zamick [18] by fitting $E2$ data in $^{206,207,209}\text{Pb}$ is $e_\nu = 0.80e$ if the states of these isotopes are described in terms of single shell-model configurations. In a later study, Thompson *et al.* [19] showed that $e_\nu = 1.1e$ reproduced the $B(E2)\uparrow$ values for $^{204,206,210}\text{Pb}$. More recently, a detailed calculation [20] has been carried out for ^{206}Pb in which two neutron holes are allowed to occupy the six lowest ($2p_{1/2}$, $2p_{3/2}$, $1f_{5/2}$, $1f_{7/2}$, $0h_{9/2}$, and $0i_{13/2}$) hole orbits. With wave functions resulting from the McGrory-Kuo interaction, the $B(E2)\uparrow$ value for ^{206}Pb is reproduced with a state-independent effective charge $e_\nu = 0.84e$. Taking an average, we obtain $e_\pi = 1.38e$ and $e_\nu = 0.91e$. This e_π value is almost the same as the Bohr-Mottelson estimate [see Eq. (5)] for these nuclei (which all have $Z A^{-1} \approx 0.4$), but this e_ν value implies $\varepsilon = 2.3$, which is slightly higher than $\varepsilon = 2.1$, deemed reasonable in the preceding paragraph.

Problems involved in estimating effective charges via perturbation theory have been reviewed by Yoshida and Zamick [18]. They support the expectation that $\alpha_\nu > \alpha_\pi$ (or $\varepsilon > 1$), but do not provide definite estimates. With information contained in the intrinsic state generated by the UWSM, we can obtain a nonperturbative estimate of ε by equating Q_0 expressed in two different ways [Eqs. (2) and (3)] and using Eq. (5). We write

$$\begin{aligned} Q_0 &= e(Q_\pi^c + Q_\nu^v) \\ &= e[(1 + Z A^{-1})Q_\pi^v + Z A^{-1}\varepsilon Q_\nu^v], \end{aligned} \quad (6)$$

which, when solved for ε , gives

$$\varepsilon = (Q_\pi^c - Z A^{-1}Q_\pi^v) / Z A^{-1}Q_\nu^v. \quad (7)$$

We will evaluate ε for selected nuclei in the next section.

Effective charges that simulate coherent quadrupole polarization of the core should not depend on the choice of configuration subspace chosen within a major shell to describe a given nucleus. We expect, however, some differences between effective charges for valence nucleons in different single-particle states. These differences have been ignored in Eq. (3). Mass quadrupole moments do depend on the configuration space of valence nucleons, and Q_π^v (Q_ν^v) values will vary depending on model assumptions. To compare with experiments, we modify Eq. (3) as

$$Q_0 = C_{\text{model}}[e_\pi Q_\pi^v + e_\nu Q_\nu^v] \quad (8)$$

and Eq. (1) as

$$B(E2)\uparrow = (5/16\pi)C_{\text{model}}^2[e_\pi Q_\pi^v + e_\nu Q_\nu^v]^2. \quad (9)$$

It is convenient to express quadrupole moments (as we have done throughout this paper) in units of the oscillator size parameter α^2 ($=\hbar/M\omega$), where M is the nucleon mass and $\hbar\omega = 41 A^{-1/3}$ MeV. The numerical value of α^2 is $0.0101 A^{1/3} b$. Effective charges are given by Eq. (5). In the chosen units, Eq. (9) becomes

$$\begin{aligned} B(E2)\uparrow &= (1.02 \times 10^{-5}) A^{2/3} C_{\text{model}}^2 \\ &\times [(1 + Z A^{-1})Q_\pi^v + (Z A^{-1}\varepsilon)Q_\nu^v]^2 e^2 b^2, \end{aligned} \quad (10)$$

with C_{model} and ε as adjustable parameters [21].

In previous papers [2,12], we wrote Eq. (10) in a slightly different form as

$$\begin{aligned} B(E2)\uparrow &= (1.02 \times 10^{-5}) A^{2/3} C_{\text{model}}^2 \\ &\times [Q_\pi^v + (e_\nu/e_\pi)Q_\nu^v]^2 e^2 b^2 \end{aligned} \quad (11)$$

and treated C_{model} (which also absorbs e_π) and e_ν/e_π as parameters whose fitted values were then given in Table I of Ref. [12]. Comparison of this equation with Eq. (10) shows that we have now introduced effective charges explicitly. If the same effective charges are now used with different models, C_{model} of Eq. (10) will reflect model assumptions concerning only the mass quadrupole moments.

We use Eq. (10) with both the SSANM and PSM as follows. Parameter ε is varied from 1.0 to 3.2. For each value of ε , the optimum normalization constant C_{model} (and its uncertainty) is obtained by a least-squares fit of calculated $B(E2)\uparrow$ values to measured ones. If the model space and assumptions are valid, we should find $C_{\text{model}} = 1$ for an agreed upon value of ε . This is the key procedure that we have adopted.

Finally, contributions of valence nucleons in abnormal-parity (a) states to the intrinsic electric (e) and mass (m) quadrupole moments are expressed by fractions f defined as follows. In the UWSM

$$f_a^e = eQ_\pi^{v,a} / eQ_\pi \quad (12)$$

and

$$f_a^m = (Q_\pi^{v,a} + Q_\nu^{v,a}) / (Q_\pi + Q_\nu), \quad (13)$$

where $Q_\pi^{v,a}$ ($Q_\nu^{v,a}$) is the total mass quadrupole moment of valence protons (neutrons) in abnormal-parity states and Q_π (Q_ν) is the total mass quadrupole moment of *all* protons (neutrons). In the SSANM

$$f_a^e = (e_\pi Q_\pi^{v,a} + e_\nu Q_\nu^{v,a}) / (e_\pi Q_\pi^v + e_\nu Q_\nu^v) \quad (14)$$

and

$$f_a^m = (Q_\pi^{v,a} + Q_\nu^{v,a}) / (Q_\pi^v + Q_\nu^v), \quad (15)$$

where Q_π^v (Q_ν^v) is the total mass quadrupole moment of *all valence* protons (neutrons). (In the SSANM the core nucleons, by definition, have zero quadrupole moment.) When calculating Q values, we have, throughout this paper, ignored the influence of pairing correlations.

III. UNIVERSAL WOODS-SAXON MODEL

This model [4] calculates the equilibrium deformation of a nucleus by minimizing the energy of its intrinsic state as a function of the shape parameters β_2 and β_4 of a Woods-Saxon potential. The total energy of all nucleons is expressed as a sum of a macroscopic contribution $E_{\text{macro}}(Z, N, \beta_2, \beta_4)$ calculated using the liquid-drop model

and a microscopic contribution $E_{\text{micro}}(Z, N, \beta_2, \beta_4)$ representing the Strutinsky shell correction together with pairing correction. The Woods-Saxon potential is specified by ten (constant) parameters whose values are given in Refs. [4] and [13].

Our interest here is to use the UWSM for three purposes: (a) Calculate parameter ε [via Eq. (7)] for $^{144}\text{Ce}_{86}$ and $^{222}\text{Ra}_{134}$, which are light nuclei in the rare-earth and actinide regions, respectively, for which this model gives a prolate equilibrium intrinsic state that has a minimum number of nucleons in abnormal-parity states. (b) Calculate abnormal fractions of the total electric and mass quadrupole moments [via Eqs. (12) and (13)] of highly deformed nuclei. For this we consider $^{128}\text{Ce}_{70}$, $^{168}\text{Er}_{100}$, and $^{250}\text{Cf}_{152}$ because their measured $B(E2)\uparrow$ values are among the largest in three different regions [$50 \leq Z \leq 82$, $50 \leq N \leq 82$ (tin region); $50 \leq Z \leq 82$, $82 \leq N \leq 126$ (rare-earth region); and $82 \leq Z \leq 126$, $126 \leq N \leq 184$ (actinide region)]. (c) Determine the extent to which deformed states of abnormal parity in the valence shell contain the spherical high- j intruder states of the shell. To do so we examine in deformed nuclei the structure of the deformed $|k| = \frac{1}{2}, \frac{3}{2}, \text{ and } \frac{5}{2}$ states originating from the high- j intruder states.

A. Effective charges

We have calculated the properties of the intrinsic states of ^{144}Ce and ^{222}Ra needed to determine ε and listed

them in Table I. The first part of this table gives the mass quadrupole moments Q_{π}^c and Q_{ν}^c of protons and neutrons, respectively, in states belonging to the shell-model core. Thus, for $^{222}\text{Ra}_{134}$, $Q_{\pi}^c = 53.1$ is the sum of mass quadrupole moments of 82 protons in the deformed states arising from the $1s, 1p, 1d-2s, 1f-2p-1g_{9/2}, \text{ and } 1g_{7/2}-2d-3s-1h_{11/2}$ shells. In the second part, we list values of $|k| = |\langle j_z \rangle|$ and corresponding mass quadrupole moments $q_k^i = \langle k, i | q_0^2 | k, i \rangle$ for valence nucleons. Label i denotes different states with same k , and $q_0^2 = \sqrt{16\pi/5} r^2 Y_0^2$ is the single-particle mass quadrupole moment operator. In $^{222}\text{Ra}_{134}$ six valence protons occupy states with $k^{\pi} = \pm \frac{1}{2}^{-}, \pm \frac{3}{2}^{-}, \text{ and } \pm \frac{1}{2}^{-}$, while eight valence neutrons occupy states with $k^{\pi} = \pm \frac{1}{2}^{+}, \pm \frac{1}{2}^{+}, \pm \frac{3}{2}^{+}, \text{ and } \pm \frac{1}{2}^{-}$, the last of which is an abnormal-parity state. In the third part, we list the $Q_{\pi(\nu)}^v$ value for valence protons (neutrons) obtained by summing the q_k^i values and then split this $Q_{\pi(\nu)}^v$ value into normal ($Q_{\pi(\nu)}^{v,n}$) and abnormal ($Q_{\pi(\nu)}^{v,a}$) contributions. In the last part, we give values of ε calculated via Eq. (7) and of f_a^e and f_a^m calculated via Eqs. (12) and (13), respectively. The values of 2.1 (^{144}Ce) and 1.8 (^{222}Ra) for ε deduced from the UWSM are close to the adopted value of 2.1, thereby confirming that our choice in Sec. II is reasonable indeed. (Effective charges e_{π}, e_{ν} for valence particles implied by the UWSM are 1.40, 0.85 for ^{144}Ce and 1.40, 0.71 for ^{222}Ra .)

TABLE I. Quadrupole moments (in units of $\alpha^2 = 0.0101 A^{1/3}$ b) of selected barely deformed nuclei according to the UWSM.

$^{144}\text{Ce}_{86}$ $\beta_2 = 0.112, \beta_4 = 0.024$				$^{222}\text{Ra}_{134}$ $\beta_2 = 0.112, \beta_4 = 0.056$			
$Q_{\pi}^c = 27.7$		$Q_{\nu}^c = 46.4$		$Q_{\pi}^c = 53.1$		$Q_{\nu}^c = 74.5$	
protons (π)		neutrons (ν)		protons (π)		neutrons (ν)	
$ k ^{\pi}$	q_k^i	$ k ^{\pi}$	q_k^i	$ k ^{\pi}$	q_k^i	$ k ^{\pi}$	q_k^i
$\frac{1}{2}^{+}$	5.03	$\frac{1}{2}^{-}$	7.35	$\frac{1}{2}^{-}$	5.88	$\frac{1}{2}^{+}$	8.99
$\frac{3}{2}^{+}$	2.58	$\frac{3}{2}^{-}$	3.90	$\frac{3}{2}^{-}$	3.84	$\frac{1}{2}^{+}$	6.90
$\frac{1}{2}^{+}$	3.42			$\frac{1}{2}^{-}$	5.17	$\frac{3}{2}^{+}$	5.96
$\frac{5}{2}^{+}$	-0.16					$\frac{1}{2}^{-}$	7.82
$Q_{\pi}^v = 21.9$		$Q_{\nu}^v = 22.5$		$Q_{\pi}^v = 29.8$		$Q_{\nu}^v = 59.3$	
$Q_{\pi}^{v,n} = 21.9$		$Q_{\nu}^{v,n} = 22.5$		$Q_{\pi}^{v,n} = 29.8$		$Q_{\nu}^{v,n} = 43.7$	
$Q_{\pi}^{v,a} = 0$		$Q_{\nu}^{v,a} = 0$		$Q_{\pi}^{v,a} = 0$		$Q_{\nu}^{v,a} = 15.6$	
$\varepsilon = 2.1$				$\varepsilon = 1.8$			
$f_a^e = 0$				$f_a^e = 0$			
$f_a^m = 0$				$f_a^m = 0.07$			

TABLE II. Quadrupole moments (in units of $\alpha^2 = 0.0101 A^{1/3} b$) of selected highly deformed nuclei according to the UWSM. The quadrupole moments for abnormal-parity states are underlined.

$^{128}\text{Ce}_{70}$				$^{168}\text{Er}_{100}$				$^{250}\text{Cf}_{152}$			
$\beta_2 = 0.270, \beta_4 = -0.010$				$\beta_2 = 0.287, \beta_4 = 0.000$				$\beta_2 = 0.250, \beta_4 = 0.024$			
$Q_\pi^c = 65.1$	$Q_\nu^c = 66.2$	$Q_\pi^c = 75.0$	$Q_\nu^c = 124.0$	$Q_\pi^c = 122.9$	$Q_\nu^c = 188.8$						
protons (π)	neutrons (ν)	protons (π)	neutrons (ν)	protons (π)	neutrons (ν)	protons (π)	neutrons (ν)	protons (π)	neutrons (ν)	protons (π)	neutrons (ν)
$ k ^\pi$	q_k^i	$ k ^\pi$	q_k^i	$ k ^\pi$	q_k^i	$ k ^\pi$	q_k^i	$ k ^\pi$	q_k^i	$ k ^\pi$	q_k^i
$\frac{1^+}{2}$	6.54	$\frac{1^+}{2}$	7.04	$\frac{1^+}{2}$	6.34	$\frac{1^-}{2}$	9.27	$\frac{1^-}{2}$	7.37	$\frac{1^+}{2}$	10.43
$\frac{3^+}{2}$	4.06	$\frac{1^+}{2}$	4.14	$\frac{3^+}{2}$	3.49	$\frac{1^-}{2}$	6.56	$\frac{3^+}{2}$	5.07	$\frac{3^+}{2}$	7.53
$\frac{3^+}{2}$	3.38	$\frac{3^+}{2}$	3.59	$\frac{1^+}{2}$	4.24	$\frac{3^-}{2}$	5.87	$\frac{1^+}{2}$	<u>8.25</u>	$\frac{1^+}{2}$	8.96
$\frac{1^-}{2}$	<u>7.54</u>	$\frac{1^-}{2}$	<u>7.96</u>	$\frac{1^-}{2}$	<u>7.54</u>	$\frac{1^+}{2}$	<u>9.29</u>	$\frac{1^-}{2}$	6.44	$\frac{1^-}{2}$	<u>10.08</u>
$\frac{3^-}{2}$	<u>6.61</u>	$\frac{3^-}{2}$	<u>6.61</u>	$\frac{3^-}{2}$	<u>6.35</u>	$\frac{3^+}{2}$	<u>8.14</u>	$\frac{3^+}{2}$	<u>7.24</u>	$\frac{3^-}{2}$	<u>9.11</u>
$\frac{3^+}{2}$	0.81	$\frac{3^+}{2}$	0.81	$\frac{5^+}{2}$	0.53	$\frac{3^-}{2}$	3.42	$\frac{5^-}{2}$	2.41	$\frac{3^+}{2}$	5.59
$\frac{5^-}{2}$	<u>4.53</u>	$\frac{5^-}{2}$	<u>4.53</u>	$\frac{5^-}{2}$	<u>4.46</u>	$\frac{5^-}{2}$	2.61	$\frac{5^+}{2}$	<u>5.70</u>	$\frac{5^+}{2}$	4.58
$\frac{5^+}{2}$	0.24	$\frac{5^+}{2}$	0.24	$\frac{3^+}{2}$	1.05	$\frac{5^+}{2}$	<u>6.29</u>	$\frac{3^-}{2}$	3.33	$\frac{5^-}{2}$	<u>6.20</u>
$\frac{1^+}{2}$	0.89	$\frac{1^+}{2}$	0.89	$\frac{7^-}{2}$	<u>2.08</u>	$\frac{7^-}{2}$	3.73	$\frac{7^-}{2}$	<u>5.35</u>	$\frac{7^-}{2}$	<u>5.35</u>
$\frac{7^-}{2}$	<u>1.97</u>									$\frac{1^+}{2}$	6.45
										$\frac{5^+}{2}$	2.31
										$\frac{7^+}{2}$	1.46
										$\frac{9^-}{2}$	<u>2.86</u>
$Q_\pi^v = 43.1$	$Q_\nu^v = 75.5$	$Q_\pi^v = 72.2$	$Q_\nu^v = 110.3$	$Q_\pi^v = 91.6$	$Q_\nu^v = 161.1$						
$Q_\pi^{v,n} = 28.0$	$Q_\nu^{v,n} = 33.4$	$Q_\pi^{v,n} = 31.3$	$Q_\nu^{v,n} = 62.9$	$Q_\pi^{v,n} = 49.2$	$Q_\nu^{v,n} = 93.9$						
$Q_\pi^{v,a} = 15.1$	$Q_\nu^{v,a} = 42.1$	$Q_\pi^{v,a} = 40.9$	$Q_\nu^{v,a} = 47.4$	$Q_\pi^{v,a} = 42.4$	$Q_\nu^{v,a} = 67.2$						
	$\epsilon = 1.3$		$\epsilon = 1.0$		$\epsilon = 1.4$						
	$f_a^e = 0.14$		$f_a^e = 0.28$		$f_a^e = 0.20$						
	$f_a^m = 0.23$		$f_a^m = 0.23$		$f_a^m = 0.19$						

TABLE III. Probability that low-lying abnormal-parity deformed states in different regions contain the high- j intruder state.

$ k $	$^{128}_{58}\text{Ce}_{70}$		$^{168}_{68}\text{Er}_{100}$		$^{250}_{98}\text{Cf}_{152}$	
	protons (π)	neutrons (ν)	protons (π)	neutrons (ν)	protons (π)	neutrons (ν)
	$j_{\pi}^a = h_{1/2}$	$j_{\nu}^a = h_{1/2}$	$j_{\pi}^a = h_{1/2}$	$j_{\nu}^a = i_{3/2}$	$j_{\pi}^a = i_{13/2}$	$j_{\nu}^a = j_{13/2}$
	$ C_j^a _{\pi}^2$	$ C_j^a _{\nu}^2$	$ C_j^a _{\pi}^2$	$ C_j^a _{\nu}^2$	$ C_j^a _{\pi}^2$	$ C_j^a _{\nu}^2$
$\frac{1}{2}$	0.69	0.68	0.64	0.60	0.64	0.61
$\frac{3}{2}$	0.74	0.74	0.70	0.65	0.68	0.65
$\frac{5}{2}$	0.81	0.81	0.78	0.72	0.75	0.69

B. Abnormal fractions of quadrupole moments

We next proceed to estimate abnormal fractions of the quadrupole moments for ^{128}Ce , ^{168}Er , and ^{250}Cf (see Table II, which is similar to Table I). Consider, for example, the properties of $^{168}\text{Er}_{100}$. According to the UWSM, even though only eight valence protons ($\sim 12\%$ of the total number of protons) are in abnormal-parity states, they contribute $f_a^e = 0.28$ or 28% to the total electric quadrupole moment. These eight protons together with six valence neutrons (for a total of 14 valence nucleons in abnormal-parity states representing $\sim 8\%$ of the total number of nucleons) also account for $f_a^m = 0.23$ or 23% of the total mass quadrupole moment. The corresponding f_a^e and f_a^m values for ^{128}Ce and ^{250}Cf are given in Table II. We conclude from these values that, according to the UWSM, nucleons in abnormal-parity states contribute typically $\sim 20\%$ to the deformation of highly deformed nuclei.

At first sight the low ε values deduced for these highly deformed nuclei (see Table II) appear to be at variance with the adopted $\varepsilon \approx 2.1$. In the UWSM abnormal-parity states in the valence shell acquire large quadrupole moments as a result of coherent mixing with other single-particle states with the same parity that belong to the shell above. These additional quadrupole moments lead to low ε values, which will be appropriate only for a shell model in which the entire $2\hbar\omega$ single-particle space is included for abnormal-parity states. If the quadrupole moments of nucleons in abnormal-parity states given in Table II were to be replaced by corresponding moments from a single-major-shell Nilsson model (in which abnormal-parity states are restricted to be pure single- j states) with the same k value, the resulting ε values will be closer to 2.1.

C. High- j content of abnormal-parity states

Finally, we determine for ^{128}Ce , ^{168}Er , and ^{250}Cf the content of abnormal-parity states φ_k^a that lie outside the major shell. These states can be expanded in terms of the single-particle states ψ_{jk} with definite angular momentum j as

$$\varphi_k = \sum_j C_{jk} \psi_{jk}. \quad (16)$$

The probability that a deformed state φ_k contains a spherical state ψ_{jk} with angular momentum j (with k being the projection of j along the axis of symmetry) is given by $|C_{jk}|^2$. We want to determine the probability that abnormal-parity deformed states φ_k^a in the 50–82, 82–126, and 126–184 regions contain the spherical states $1h_{11/2}$, $1i_{13/2}$, and $1j_{15/2}$, respectively. These probabilities as determined by UWSM wave functions are listed in Table III.

From Table III we see that abnormal-parity states of the UWSM, and presumably of these nuclei, contain appreciable admixture of states from the next shell. This table essentially provides an estimate of the goodness (and the limitation) of the assumption often made in practical shell models (such as the PSM or FDSM) that the structure of deformed nuclei can be well described within a model configuration space consisting of a major shell with only the high- j state as the abnormal-parity state.

IV. SINGLE-SHELL ASYMPTOTIC NILSSON MODEL

A. SSANM for three different regions

In Refs. [11] and [12], we used the ansatz that “a nucleus is as deformed as it can be in a single shell” to calculate intrinsic quadrupole moments for nuclei in different shells. If the deformation of a nucleus, and hence of the Nilsson potential, is large, the differences in the energies ε_j of the spherical single-particle states may be ignored and the deformed single-particle states φ_k^i become, to a good approximation for axially symmetric quadrupole deformation, eigenstates of the quadrupole moment operator. These eigenstates were constructed by diagonalizing the matrix $\langle \psi_{j'k} | q_0^2 | \psi_{jk} \rangle$, where ψ_{jk} are the spherical single-particle states. The eigenvalues q_k^i of this matrix for each of the eigenstates φ_k^i are just the mass quadrupole moments of these deformed single-particle states.

Table IV gives a partial list of q_k^i in three different

TABLE IV. Partial list of the quadrupole moments (in units of $\alpha^2=0.0101 A^{1/3}$ b) of the asymptotically deformed states in the SSANM. The quadrupole moments for abnormal-parity states are underlined.

50–82 shell, $j_a = h_{1/2}$		82–126 shell, $j_a = i_{13/2}$		126–184 shell, $j_a = j_{13/2}$	
$ k ^\pi$	q_k^i	$ k ^\pi$	q_k^i	$ k ^\pi$	q_k^i
$\frac{1}{2}^+$	7.4	$\frac{1}{2}^-$	9.6	$\frac{1}{2}^+$	11.7
$\frac{1}{2}^+$	3.8	$\frac{1}{2}^-$	6.2	$\frac{1}{2}^+$	8.4
$\frac{3}{2}^+$	3.5	$\frac{3}{2}^-$	5.9	$\frac{3}{2}^+$	8.2
$\frac{1}{2}^-$	<u>3.2</u>	$\frac{1}{2}^+$	<u>3.7</u>	$\frac{3}{2}^+$	5.0
$\frac{3}{2}^-$	<u>2.6</u>	$\frac{3}{2}^+$	<u>3.2</u>	$\frac{1}{2}^+$	4.6
$\frac{5}{2}^-$	<u>1.5</u>	$\frac{3}{2}^-$	2.7	$\frac{3}{2}^+$	4.5
$\frac{3}{2}^+$	0.2	$\frac{5}{2}^+$	<u>2.3</u>	$\frac{1}{2}^-$	<u>4.2</u>
$\frac{7}{2}^-$	<u>-0.1</u>	$\frac{1}{2}^-$	2.2	$\frac{3}{2}^-$	<u>3.8</u>
$\frac{1}{2}^+$	-0.2	$\frac{5}{2}^-$	2.2	$\frac{5}{2}^-$	<u>3.0</u>
$\frac{5}{2}^+$	-0.2	$\frac{7}{2}^+$	<u>0.9</u>	$\frac{7}{2}^-$	<u>1.8</u>
				$\frac{3}{2}^+$	1.6
				$\frac{1}{2}^+$	1.1
				$\frac{7}{2}^+$	1.0
				$\frac{3}{2}^+$	0.9
				$\frac{9}{2}^-$	<u>0.2</u>

shells. Abnormal-parity states are considered here as *pure* high- j states. Consequently, the quadrupole moments of the abnormal-parity $|k| = \frac{1}{2}, \frac{3}{2}, \frac{5}{2}$ states are much smaller than the quadrupole moments of corresponding states in the UWSM. Consider, for example, such states of the $i_{13/2}$ intruder in the 82–126 shell. The quadrupole moments of 3.7, 3.2, and 2.3 for these states in the SSANM (see underlined values in Table IV) are much smaller than the corresponding values of 9.29, 8.14, and 6.29 in the UWSM (see Table II). The normal-parity states, on the other hand, have similar quadrupole moments in both models. Therefore the summed $Q_\pi^{v,n}$ and $Q_\nu^{v,n}$ values contributed by nucleons in normal-parity states are similar in the UWSM and SSANM, whereas the corresponding values due to nucleons in abnormal-parity states are much greater in the UWSM than in the SSANM. It is this enhancement that accounts for the small ϵ value deduced from the UWSM (see Table II) for these nuclei.

For a nucleus with prolate deformation, the intrinsic state with the largest mass quadrupole moment is formed by sequentially putting valence nucleons (consistent with the Pauli principle) in the asymptotic Nilsson states with decreasing moments. For the few nuclei that are known experimentally or theoretically to be oblate, the states are filled in reverse order, starting with the state with the

smallest moment. We then follow the key procedure outlined in Sec. II to obtain C_{model} vs ϵ shown in Fig. 1. At $\epsilon=2.1$, which we take as a reasonable value, the C_{SSANM} values are 0.80 ± 0.07 , 1.01 ± 0.08 , and 1.00 ± 0.04 for the tin, rare-earth, and actinide regions, respectively. These normalization factors are indeed *close to unity*. If, on the other hand, ϵ is forced to be unity, the resulting C_{SSANM} values (see Fig. 1) for the tin, rare-earth and actinide regions are 0.89 ± 0.15 , 1.29 ± 0.16 , and 1.37 ± 0.06 , respectively, which would imply an overestimate of quadrupole moment in the tin region by $\sim 11\%$ and underestimates of quadrupole moment by $\sim 29\%$ and $\sim 37\%$ in the other two regions. In the tin region [see Fig. 1(a)], C_{SSANM} is not unity for any $1.0 \leq \epsilon \leq 3.2$ value unless the uncertainty in C_{SSANM} is taken into account. Even though nuclei in the “tin” region ($50 \leq Z$, $N \leq 82$) are not as deformed as they are in the rare-earth region ($50 \leq Z \leq 82$, $82 \leq N \leq 126$), we have continued to employ *asymptotic* values that tends to overpredict quadrupole moment in the tin region—hence $C_{\text{SSANM}} < 1$.

For each ϵ the percentage of the calculated $B(E2)^\uparrow$ values that overlap within one standard deviation with the measured values (when uncertainties are applied to *both* sets of values) is also shown in Fig. 1. This percentage does not depend strongly on ϵ . Therefore it is futile to rely on least-squares fits to deduce best unique values

for C_{SSANM} and ϵ simultaneously. (The same conclusion applies to other models discussed below.)

B. SSANM restricted to deformed nuclei

Because the PSM discussed in the next section treats only nuclei that are deformed, it is appropriate for later comparison to carry out another set of fits with the SSANM for a restricted set of such nuclei. The results are shown in Fig. 2. In the rare-earth region, C'_{SSANM}

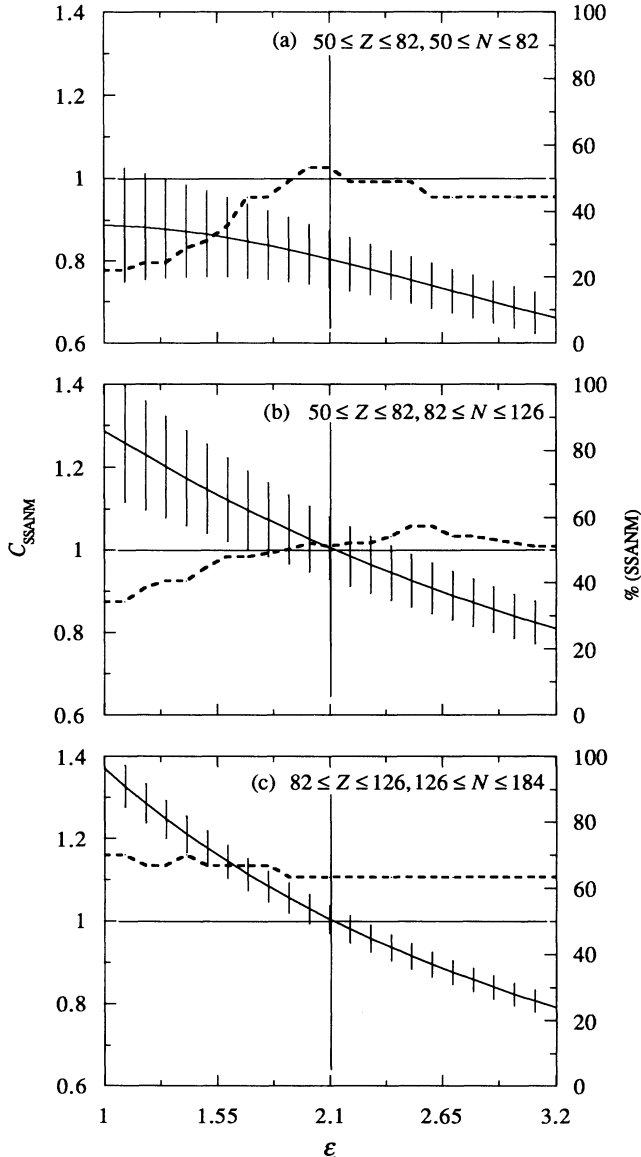


FIG. 1. Variation of the normalization constant C [see Eq. (10)] of the single-shell asymptotic Nilsson model (SSANM) with the parameter ϵ [see Eq. (5)] defining the neutron effective charge. The proton effective charge is taken as $e[1+(Z/A)]$. Solid curves (with error bars) give C (and its uncertainty) for the (a) tin region [which contains 45 nuclei with measured $B(E2)\uparrow$ values], (b) rare-earth region (96 nuclei), and (c) actinide region (30 nuclei). Dashed curves denote the percentage of cases where calculated $B(E2)\uparrow$ values overlap within one standard deviation with measured values.

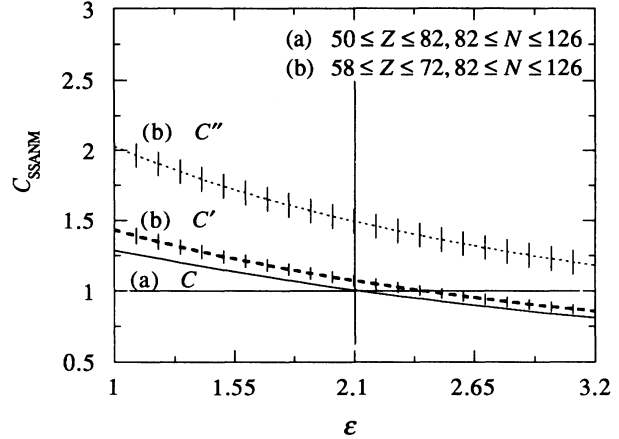


FIG. 2. Variation of the normalization constant C (solid line), C' (dashed line) or C'' (dotted line) of the SSANM with the parameter ϵ . The solid line is carried over from Fig. 1(b), the dashed line (with error bars) denotes fits restricted to 38 highly deformed nuclei in the Ce–Hf region with measured $B(E2)\uparrow$ values, and the dotted line (with error bars) denotes fits to the same number of nuclei while contributions of nucleons in abnormal-parity states are deliberately switched off in calculating model $B(E2)\uparrow$ values.

($\epsilon=2.1$) is now 1.07 ± 0.11 , slightly larger than 1.01 ± 0.08 found earlier. In the actinide region, omitting the only nucleus ^{218}Ra , which does not have a rotational spectrum, from the set of nuclei included in the previous fit [see Fig. 1(c)] have negligible influence either on the fit or on the conclusion that the SSANM gives correct $B(E2)\uparrow$ predictions in the rare-earth and actinide regions with $\epsilon=2.1$ and $C_{\text{SSANM}}\approx 1$.

We now calculate abnormal fractions of the quadrupole moments for ^{128}Ce , ^{168}Er , and ^{250}Cf considered in Sec. III. We use values given in Table IV to calculate the various quantities (see Table V) that go into Eqs. (14) and (15) that determine these fractions. The resulting f_a^e and f_a^m values (with $\epsilon=2.1$) for these nuclei are given at the

TABLE V. Abnormal fractions f of electric and mass quadrupole moments (in units of α^2) of selected nuclei in the SSANM for $\epsilon=2.1$.

	$^{128}_{58}\text{Ce}_{70}$	$^{168}_{68}\text{Er}_{100}$	$^{250}_{98}\text{Cf}_{152}$
Q_{π}^v	35.8	43.8	71.6
$Q_{\pi}^{v,n}$	29.4	29.4	53.2
$Q_{\pi}^{v,a}$	6.4	14.4	18.2
Q_{ν}^v	43.4	76.0	117.8
$Q_{\nu}^{v,n}$	29.0	57.6	92.2
$Q_{\nu}^{v,a}$	14.4	18.4	25.6
f_a^e	0.25	0.28	0.24
f_a^m	0.26	0.27	0.23

bottom of Table V. We conclude from these values (which are relatively insensitive to ϵ) that, according to the SSANM, nucleons in abnormal-parity states contribute typically $\sim 25\%$ (compared with $\sim 20\%$ in the UWSM) to the deformation of highly deformed nuclei.

Also, for later comparison, we introduce artificially into the SSANM the assumption that nucleons in abnormal-parity states do not contribute to deformation. This is done simply by removing the amount contributed by nucleons in abnormal-parity states from the total intrinsic quadrupole moments of valence protons and valence neutrons for each nucleus. These smaller quadrupole moments are then substituted into Eq. (10), and the resulting variation of C''_{SSANM} vs ϵ is shown in Fig. 2. We note that $C''_{\text{SSANM}}(\epsilon=2.1)$ is now 1.49 ± 0.09 . In other words, any relegation of abnormal-parity states to a minor role and the resulting underestimation of quadrupole moments can be offset by an increase in the overall normalization constant.

V. PSEUDO-SU(3) MODEL

A. Introduction

Because interest in the pseudo-SU(3) model with symplectic extensions [9] has been revived in recent years as a useful microscopic model for understanding collective rotations of deformed and superdeformed nuclei, we recapitulate briefly the main features and assumptions of this model and explain how $B(E2)\uparrow$ values can be readily calculated.

Elliott [22] showed that the dominance of the quadrupole-quadrupole (qq) component of an effective interaction between nucleons, together with a harmonic-oscillator description of single-particle states, leads to a nuclear Hamiltonian with SU(3) symmetry having rotational spectra. This single-oscillator-shell symmetry is broken by a spin-orbit interaction and is rendered useless as a practical truncation scheme in calculations for heavy nuclei in which this interaction pushes down the highest- j state of the shell to intrude into and become part of the lower major shell.

The pseudo-SU(3) model (PSM) [9] starts with the observation that *normal-parity* states in the 50–82, 82–126, and 126–184 shells occur in “approximately” degenerate doublets. For example, in the 50–82 major shell, normal-parity single-particle states are the $1g_{7/2}$, $2d_{5/2}$, $2d_{3/2}$, and $3s_{1/2}$ states. The $1g_{7/2}$ and $2d_{5/2}$ states are close in energy and so are the $2d_{3/2}$ and $3s_{1/2}$ states. Thus the states with $j=l+\frac{1}{2}$ and $j=l+2-\frac{1}{2}$ are found to be approximately degenerate. The pseudoscheme introduces a pseudo angular momentum \tilde{l} defined as the average of the orbital angular momenta of the degenerate doublet: $\tilde{l}=l+1$. The $1g_{7/2}, 2d_{5/2}$ doublet is considered to be the $\tilde{f}_{7/2}, \tilde{f}_{5/2}$ pseudo spin-orbit doublet with $\tilde{l}=3$ and the $2d_{3/2}, 3s_{1/2}$ doublet to be the $\tilde{p}_{3/2}, \tilde{p}_{1/2}$ doublet with $\tilde{l}=1$. Thus the four normal-parity states with oscillator quantum number $N=4$ and $l=0, 2$, and 4 in the 50–82 major shell are associated with the four states with a pseudo oscillator quantum number $\tilde{N}=N-1=3$ and pseudo angular momenta $\tilde{l}=1$ and 3 .

The spherical single-particle shell-model Hamiltonian is often written as [6]

$$\mathcal{H} = \mathcal{H}_0 + Cl \cdot s + Dl^2. \quad (17)$$

The unitary transformation from the real to the pseudo-states maps the Hamiltonian \mathcal{H} into $\tilde{\mathcal{H}}$ given by [9]

$$\tilde{\mathcal{H}} = \tilde{\mathcal{H}}_0 + (4D - C)\tilde{l} \cdot \tilde{s} + D\tilde{l}^2 + (\hbar\omega + 2D - C). \quad (18)$$

Because pseudo spin-orbit doublets with $\tilde{j} = \tilde{l} \pm \frac{1}{2}$ are observed to be approximately degenerate ($4D \approx C$ in terms of Nilsson parameters), the normal-parity part of a major shell with a large spin-orbit interaction is transformed into a pseudo oscillator shell with a small spin-orbit interaction. In addition, detailed calculations have shown [9] that the dominant qq interaction in the normal space is also transformed into a dominant pseudo qq interaction with small corrections. A many-body Hamiltonian with effective $Q \cdot Q$ interaction,

$$\mathcal{H} = \sum_i h_0^{(i)} + C \sum_i l_i \cdot s_i + D \sum_i l_i^2 - \frac{1}{2} \chi Q \cdot Q, \quad (19)$$

is thus transformed into a pseudo Hamiltonian:

$$\tilde{\mathcal{H}} = \tilde{\mathcal{H}}_0 + D \sum_i \tilde{l}_i^2 - \frac{1}{2} \tilde{\chi} \tilde{Q} \cdot \tilde{Q} + \text{corrections}, \quad (20)$$

which has pseudo-SU(3) symmetry to a good approximation. The Hamiltonian $\tilde{\mathcal{H}}$ takes into account, analytically, the strong quadrupole correlations among normal-parity states of a major shell.

For further simplicity the PSM assumes that nucleons in an abnormal-parity high- j state are coupled to states with definite seniority. Such an assumption would be reasonable if the $(2j+1)$ substates of the high- j state were approximately degenerate as in spherical nuclei. However, at large deformations, this assumption may not be *a priori* reasonable because the splitting of these substates is quite large. Nevertheless, it does greatly simplify computations.

The yrast band of a deformed nucleus is, in the simplest version of this model, constructed by coupling the pseudo-SU(3) band belonging to the *highest* representation $[\lambda, \mu]$ of nucleons in normal-parity states to the *seniority-zero* state of nucleons in an abnormal-parity intruder state. The PSM uses the Nilsson scheme to determine the distribution of valence nucleons among normal- and abnormal-parity states.

Our current interest is limited to $B(E2)\uparrow$ given in the PSM by the representation $[\lambda, \mu]$ associated with the yrast band. We describe in the following subsections how this representation is obtained. We follow this with a detailed comparison between measured $B(E2)\uparrow$ values and those calculated with the PSM and FDSM because both models treat nucleons in abnormal-parity states the same way for similar reasons. In addition, for the deformed nuclei under consideration, both models assume SU(3) symmetry for nucleons in normal-parity states. However, the underlying structure of the SU(3) symmetry and the specific SU(3) representations which the two models as-

cribe to a given nucleus are, of course, different. Therefore it would be interesting to see whether the $B(E2)^\dagger$ data can distinguish between these two models.

B. Determining the SU(3) representation

First, we consider real SU(3) in harmonic-oscillator shells [22,23]. In the absence of a spin-orbit interaction, space-spin single-particle states belonging to an oscillator shell with quantum number N are labeled in the spherical basis by the quantum numbers $nlm_l m_s$, where $m_l = \langle l_z \rangle$, $m_s = \langle s_z \rangle$, and $N = 2(n-1) + l$. Allowed n and l values are $n = 1, 2, \dots, N-1$ and $l = N, N-2, \dots, 1$ or 0 . To determine SU(3) representations, it is better to relabel these states in a deformed basis by the number of quanta, n_3, n_1 , and n_2 , along the body-fixed z', x' , and y' axes and $k_s = \langle s_z \rangle$. Here $N = n_3 + n_1 + n_2$, and a state labeled by N and n_3 has a mass quadrupole moment $q = 3n_3 - N$. It is further convenient to relabel these states with definite values of $k_l = \langle l_z \rangle$ and, hence, of total $k = \langle j_z \rangle = k_l + k_s$. For given N and n_3 values, allowed k_l values are $N - n_3, N - n_3 - 2, \dots, -(N - n_3)$. The mass quadrupole moment is again given by $q_k^i = 3n_3 - N$, where i labels different states with the same k . The states now carry the quantum numbers $n_3 q_k^i k_l k_s$. The space parts of the single-particle states in a major shell N (see Table VI for $N=3$) labeled by $nlm_l, n_3 n_1 n_2$, and $n_3 q_k^i k_l k_s$ can be expressed as linear combinations of each other.

An intrinsic state is obtained by putting particles sequentially in $n_3 n_1 n_2$ states with the largest available value of n_3 , and hence of q_k^i , taking into account the Pauli principle. Each state can be occupied by two nucleons with spin projections $k_s = \pm \frac{1}{2}$. Let N_3, N_1, N_2 represent the total number of quanta along the z', x', y' axes for these particles. The SU(3) representation $[\lambda, \mu]$ of this intrinsic state is given by $\lambda = N_3 - N_1$ and $\mu = N_1 - N_2$. We

illustrate the procedure with an example. The intrinsic state of six particles in the $N=3$ shell is obtained by putting them in the first three states listed in Table VI. Therefore $N_3 = 2[3+2+2] = 14$, $N_1 = 2[0+1+0] = 2$, and $N_2 = 2[0+0+1] = 2$. This state has the SU(3) quantum numbers $[\lambda, \mu] = [12, 0]$. If λ or $\mu = 0$, the intrinsic state is axially symmetric; if $\mu = 0$, it is prolate; if $\lambda = 0$, it is oblate; if $\lambda, \mu \neq 0$ and $\lambda > \mu$, it is prolate triaxial; and if $\lambda, \mu \neq 0$ and $\lambda < \mu$, it is oblate triaxial. The most prolate state of eight particles in the $N=3$ shell has $N_3 = 16$, $N_1 = 6$, and $N_2 = 2$ with $[\lambda, \mu] = [10, 4]$. This state is prolate triaxial. By constructing a table for $N=4$ similar to Table VI, it is easy to show that the most prolate six- and eight-particle states in the $N=4$ shell will have $[\lambda, \mu] = [18, 0]$ and $[18, 4]$, respectively.

Now we connect this to the determination of the SU(3) representations $[\lambda, \mu]$ in the PSM. Recall that in this model normal-parity $1g_{7/2}, 2d_{5/2}, 2d_{3/2}$, and $3s_{1/2}$ states (the $N=4$ oscillator part of the 50–82 major shell) are mapped into $\tilde{f}_{7/2}, \tilde{f}_{5/2}, \tilde{p}_{3/2}$, and $\tilde{p}_{1/2}$ states (the full $\tilde{N}=3$ pseudo oscillator shell). The SU(3) representations for $\tilde{N}=3$ and $N=3$ shells are the same. Hence we can use Table VI (for $N=3$) to determine the most prolate pseudo-SU(3) representations $[\lambda, \mu]$ for particles in normal-parity states in the 50–82 major shell. In general, the SU(3) representations for a given number of particles in the pseudo oscillator shell with quantum number \tilde{N} are the same as those for the same number of particles in the oscillator shell with quantum number $N = \tilde{N}$. Thus, for six and eight particles in normal-parity states of the 50–82 major shell ($\tilde{N}=3$), the pseudo-SU(3) representations are $[12, 0]$ and $[10, 4]$, respectively. Similarly, for six and eight particles in normal-parity states of the 82–126 shell ($\tilde{N}=4$), the pseudo-SU(3) representations for the most prolate states are $[18, 0]$ and $[18, 4]$, respectively.

TABLE VI. Different ways of labeling single-particle states of the $N=3$ shell.

Spherical basis			Deformed basis			Deformed basis		
n	ℓ	m	n_3	n_1	n_2	n_3	q	k_l
1	3	3	3	0	0	3	6	0
1	3	2	2	1	0	2	3	1
1	3	1	2	0	1	2	3	-1
1	3	0	1	2	0	1	0	2
1	3	-1	1	1	1	1	0	0
1	3	-2	1	0	2	1	0	-2
1	3	-3	0	3	0	0	-3	3
2	1	1	0	2	1	0	-3	1
2	1	0	0	1	2	0	-3	-1
2	1	-1	0	0	3	0	-3	-3

For heavy, deformed nuclei in the rare-earth region, normal-parity states of protons and neutrons belong to the pseudo oscillator shells $\tilde{N}_\pi=3$ and $\tilde{N}_\nu=4$, respectively. For the actinides they belong to the $\tilde{N}_\pi=4$ and $\tilde{N}_\nu=5$ pseudoshells, respectively. If $[\lambda_\pi, \mu_\pi]$ and $[\lambda_\nu, \mu_\nu]$ are pseudo-SU(3) representations, the intrinsic state of the nucleus has $[\lambda, \mu] = [\lambda_\pi + \lambda_\nu, \mu_\pi + \mu_\nu]$.

The quadrupole moments for the $\tilde{N}_\pi=3$ and $\tilde{N}_\nu=4$ oscillator shells are given in Table VII. We note here that in the PSM the quadrupole moment of nucleons in the $|k| = \frac{1}{2}, \frac{3}{2}, \dots$ normal-parity states are smaller than the corresponding values in the SSANM containing the same normal-parity states. For example, in the PSM, q_k^i values are 6, 3, and 3, respectively, for $|k| = \frac{1}{2}, \frac{1}{2},$ and $\frac{3}{2}$ states in the 82–126 region compared with 9.6, 6.2, and 5.9 in the SSANM (see Table IV). Therefore, relative to the SSANM, we expect the PSM to underestimate the quadrupole moments of nucleons in normal-parity states.

TABLE VII. Spectra of the mass quadrupole moments q_k^i (in units of a^2) of the asymptotically deformed states of the $\tilde{N}=3$ and 4 pseudo oscillator shells.

$\tilde{N}=3$ shell		$\tilde{N}=4$ shell	
$ k ^\pi$	q_k^i	$ k ^\pi$	q_k^i
$\frac{1}{2}^+$	6	$\frac{1}{2}^-$	8
$\frac{1}{2}^+$	3	$\frac{1}{2}^-$	5
$\frac{3}{2}^+$	3	$\frac{3}{2}^-$	5
$\frac{1}{2}^+$	0	$\frac{1}{2}^-$	2
$\frac{3}{2}^+$	0	$\frac{3}{2}^-$	2
$\frac{5}{2}^+$	0	$\frac{5}{2}^-$	2
$\frac{1}{2}^+$	-3	$\frac{1}{2}^-$	-1
$\frac{3}{2}^+$	-3	$\frac{3}{2}^-$	-1
$\frac{5}{2}^+$	-3	$\frac{5}{2}^-$	-1
$\frac{7}{2}^+$	-3	$\frac{7}{2}^-$	-1
		$\frac{1}{2}^-$	-4
		$\frac{3}{2}^-$	-4
		$\frac{5}{2}^-$	-4
		$\frac{7}{2}^-$	-4
		$\frac{9}{2}^-$	-4

C. Quadrupole moment of the intrinsic state

In the real oscillator SU(3) model, the expectation value of the mass quadrupole moment Q of the most deformed intrinsic state belonging to a representation $[\lambda, \mu]$ is given by $Q = (2\lambda + \mu)$. Because the real \leftrightarrow pseudo unitary transformation does not affect radial motion, the same relation gives the Q of the intrinsic state belonging to a pseudo-SU(3) representation $[\lambda, \mu]$. We showed in the previous subsection that the representation is $[12, 0]$ for the six-particle state in the $\tilde{N}=3$ shell; therefore, the total Q is 24. The same value of $Q = 2(6+3+3) = 24$ is obtained by summing q_k^i of the occupied single-particle states listed in Table VII.

D. Pseudo-SU(3) representation for a given nucleus

For a nucleus under consideration, its SU(3) representation in the PSM is determined only by the number of nucleons in normal-parity states N_n which can be obtained by appealing to the Nilsson diagram. The prescription is to look up the sequence of Nilsson states corresponding to a deformation parameter in the range $\beta_2 \sim 0.20-0.25$, put in valence nucleons in these states, and count the number N_n and N_a of nucleons that occupy normal- and abnormal-parity states. Abnormal-parity states play no further role. The appropriate representations for protons and neutrons in normal-parity states, $[\lambda_\pi, \mu_\pi]$ and $[\lambda_\nu, \mu_\nu]$, are then coupled to the highest resultant representation $[\lambda, \mu]$. The mass quadrupole moment Q is then simply $2\lambda + \mu$. A similar procedure is also used in the FDSM.

In Table VIII we have listed N_n and N_a values for a given number N of valence nucleons in three different shells. In constructing this table we considered only the Nilsson states belonging to the single-particle states within the major shell and ignored other states intruding from the shells above and below the shell under consideration. In Table VIII we have also listed the pseudo-SU(3) representation corresponding to the number N_n of nucleons in normal-parity states and the intrinsic quadrupole moment Q for this representation.

We use the representation $[\lambda, \mu]$ listed in Table VIII to determine the final SU(3) representations for different nuclei. Consider, for example, $^{154}\text{Gd}_{90}$. The representation $[\lambda_\pi, \mu_\pi]$ for 14 protons in the 50–82 shell is $[10, 4]$ and $[\lambda_\nu, \mu_\nu]$ for 8 neutrons in the 82–126 shell is $[18, 0]$. The overall pseudo-SU(3) representation $[\lambda, \mu]$ for the yrast band of ^{154}Gd [24] is thus $[28, 4]$ and $Q = 60$. The intrinsic quadrupole moments Q_π and Q_ν of the protons and neutrons for this nucleus are separately 24 and 36, respectively.

E. $B(E2)\uparrow$ values: Comparison with measurements

To calculate $B(E2)\uparrow$ values given by the PSM, we substitute into Eq. (10) the Q_π^v and Q_ν^v values for different nuclei following the procedure just described for ^{154}Gd . As before, we vary ϵ and determine C_{PSM} by a least-squares

TABLE VIII. Partition of N valence nucleons into N_n in normal-parity and N_a in abnormal-parity states. The SU(3) representations $[\lambda, \mu]$ corresponding to N_n and the resulting intrinsic quadrupole moments $Q=2\lambda+\mu$ (in units of α^2) are listed.

N	N_n	N_a	$[\lambda, \mu]$	Q	N	N_n	N_a	$[\lambda, \mu]$	Q
50 – 82 shell (neutrons and protons)					82 – 126 shell (protons) (continued)				
2	2		[6,0]	12	14	8	6	[18,4]	40
4	4		[8,2]	18	16	10	6	[20,4]	44
6	6		[12,0]	24	18	10	8	[20,4]	44
8	6	2	[12,0]	24	20	12	8	[24,0]	48
10	6	4	[12,0]	24	22	12	10	[24,0]	48
12	6 or 8	6 or 4	[12,0] or [10,4]	24 or 24	24	14	10	[20,6]	46
14	8	6	[10,4]	24	26	16	10	[18,8]	44
16	10	6	[10,4]	24	28	16 or 18	12 or 10	[18,8] or [18,6]	44 or 42
18	10	8	[10,4]	24	30	18	12	[18,6]	42
20	12	8	[12,0]	24	32	20	12	[20,0]	40
22	14	8	[6,6]	18	34	22	12	[12,8]	32
24	16 or 14	8 or 10	[2,8] or [6,6]	12 or 18	36	24	12	[6,12]	24
26	16	10	[2,8]	12	38	24	14	[6,12]	24
28	16	12	[2,8]	12	40	26	14	[2,12]	16
30	18	12	[0,6]	12	42	28	14	[0,8]	8
32	20	12	[0,0]	0	44	30	14	[0,0]	0
82 – 126 shell [neutrons]					126 – 184 shell [neutrons]				
2	2	0	[8,0]	16	2	2	0	[10,0]	20
4	4	0	[12,2]	26	4	4	0	[16,2]	34
6	6	0	[18,0]	36	6	6	0	[24,0]	48
8	6	2	[18,0]	36	8	6	2	[24,0]	48
10	6	4	[18,0]	36	10	6	4	[24,0]	48
12	8	4	[18,4]	40	12	8	4	[26,4]	56
14	8	6	[18,4]	40	14	8	6	[26,4]	56
16	10	6	[20,4]	44	16	10	6	[30,4]	64
18	10	8	[20,4]	44	18	10	8	[30,4]	64
20	12	8	[24,0]	48	20	12	8	[36,0]	72
22	14	8	[20,6]	46	22	14	8	[34,6]	74
24	16	8	[18,8]	44	24	16	8	[34,8]	76
26	16	10	[18,8]	44	26	16	10	[34,8]	76
28	18	10	[18,6]	42	28	18	10	[36,6]	78
30	20	10	[20,0]	40	30	20	10	[40,0]	80
32	22	10	[12,8]	32	32	22	10	[34,8]	76
34	22	12	[12,8]	32	34	22	12	[34,8]	76
36	24	12	[6,12]	24	36	24	12	[30,12]	72
38	24	14	[6,12]	24	38	26	12	[28,12]	68
40	26	14	[2,12]	16	40	26	14	[28,12]	68
42	28	14	[0,8]	8	42	28	14	[28,8]	64
44	30	14	[0,0]	0	44	30	14	[30,0]	60
					46	32	14	[20,10]	50
					48	34	14	[12,16]	40
					50	34	16	[12,16]	40
2	2	0	[8,0]	16	52	36	16	[6,18]	30
4	2 or 4	2 or 0	[8,0] or [12,2]	16 or 26	54	38	16	[2,16]	20
6	4	2	[12,2]	26	56	40	16	[0,10]	10
8	4	4	[12,2]	26	58	42	16	[0,0]	0
10	6	4	[18,0]	36					
12	6	6	[18,0]	36					

fit to the measured values. The results are shown in Fig. 3. If e_π is taken as $e[1+(Z/A)]$, C_{PSM} is *greater than unity* for $1 \leq \epsilon \leq 3.2$; only for an unreasonable value of ϵ does C_{PSM} approach unity. Alternatively, if $\epsilon=2.1$, agreement between the PSM and measured values is obtained with the help of $C_{\text{PSM}}=1.85 \pm 0.08$ and $C_{\text{PSM}}=1.66 \pm 0.03$, respectively, for the rare-earth and actinide regions. These values are to be compared with $C'_{\text{SSANM}}=1.07 \pm 0.04$ and $C'_{\text{SSANM}}=1.00 \pm 0.04$, respectively, obtained earlier. We conclude that the PSM underestimates mass quadrupole moments by $\sim 85\%$ in the rare-earth region and $\sim 66\%$ in the actinide region.

In Sec. IV B we generated a C'_{SSANM} vs ϵ curve (see dotted curve in Fig. 2) for selected rare-earth nuclei with a special SSANM in which the quadrupole moments of nucleons in abnormal-parity states were deliberately set to zero to mimic the assumption of the PSM. This curve is reproduced in Fig. 4 as a dotted curve. Comparison of the two curves shows that the PSM also underestimates the electric quadrupole moments of nucleons in normal-parity states by about 35% compared with the SSANM. This loss can be absorbed in the definition of the PSM quadrupole operator [25]. The remaining $\sim 50\%$ reduction in quadrupole moments is, therefore, due to the assumption of the PSM that nucleons in abnormal-parity

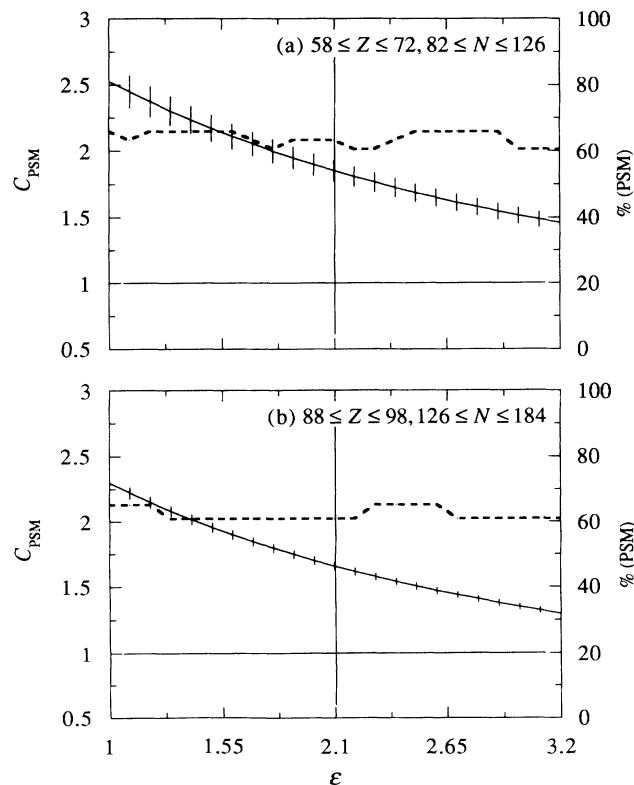


FIG. 3. Variation of the normalization constant C [see Eq. (10)] of the pseudo-SU(3) model (PSM) with the parameter ϵ . Solid curves (with error bars) give C (and its uncertainty) for highly deformed nuclei in the (a) rare-earth region (38 nuclei) and (b) actinide region (23 nuclei). Dashed curves denote the percentage of cases where calculated $B(E2)\uparrow$ values overlap within one standard deviation with measured values.

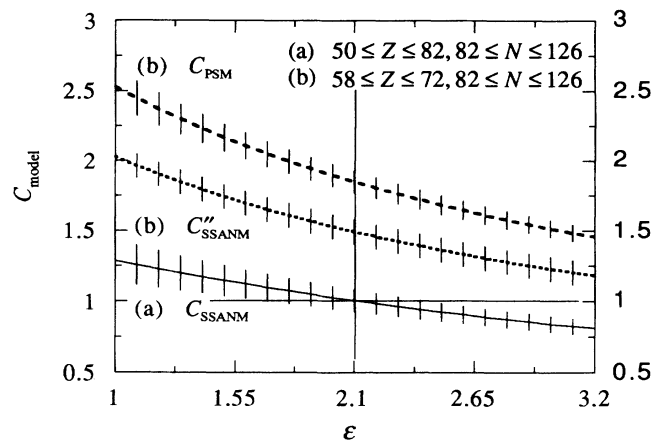


FIG. 4. C_{PSM} curve of Fig. 3(a) is reproduced here as a dashed line and compared with C_{SSANM} (solid line) from Fig. 1(b) and C''_{SSANM} (dotted line) from Fig. 2.

states do not contribute to it.

For deformed nuclei in the rare-earth region, we required $C_{\text{PSM}}=1.85$ to obtain good agreement between the PSM and measured $B(E2)\uparrow$ values if the effective charges were chosen as $e_\pi \approx 1.41e$ and $e_\nu \approx 0.86e$. On the other hand, Castaños, Draayer, and Leschber [26] have shown that both good agreement and $C_{\text{PSM}} \approx 1$ can be obtained with a different choice of effective charges, $e_\pi = 2e$ and $e_\nu = e$. The importance of agreeing *ab initio* as to what the effective charges should be becomes immediately clear—otherwise, there is too much flexibility (three adjustable parameters) in making comparisons between theory and experiment, and little physical insight is gained. Especially, the role played by nucleons in abnormal-parity states can be evaluated *only* if different shell models employ, as we have done, the same effective charges. Based as they are on quite general arguments (see Secs. II and III), plausibly our e_π and e_ν values and certainly our procedure of varying ϵ are preferable in any intercomparison of the results of different models within a single-major-shell configuration space.

The pseudosymplectic scheme [25] of extending the single-major-shell PSM allows explicitly for deformation of the core, thereby obviating the need for effective charges, but it still assumes that valence (as well as core) nucleons in abnormal-parity states do not contribute any quadrupole moment. We have shown [12,13] that the UWSM, which also has no effective charges, is successful in reproducing nuclear deformation without the need for significant renormalizations. This model gives equal weights to nucleons in normal- and abnormal-parity states. Hence the key assumption concerning nucleons in abnormal-parity states in the pseudosymplectic scheme should lead to a loss of quadrupole moment, certainly relative to the UWSM, which has to be somehow compensated for. In the case of $B(E2)\uparrow$ for ^{238}U , good agreement between theory and experiment has been obtained [25] within this scheme by introducing appropriate vertical $n\hbar\omega$ mixing—a procedure that completely obscures

the role played by nucleons in abnormal-parity states, which is the central theme of this paper.

F. $B(E2)\uparrow$ values: Comparison with FDSM values

Both the PSM and FDSM operate within the same model space of a single major shell. In their simplest versions, both assume that nucleons in abnormal-parity states do not contribute directly to the total deformation of the nucleus. Both models rely on the Nilsson model for the apportionment of valence nucleons into normal- and abnormal-parity states. Deformed nuclei in the actinide region are treated in terms of SU(3) symmetry by both models; those in the rare-earth region are assumed to have ${}^{\pi}\text{SU}(3)\otimes{}^{\nu}\text{SU}(3)$ symmetry in the PSM and ${}^{\pi}\text{SO}(6)\otimes{}^{\nu}\text{SU}(3)$ symmetry in the FDSM. Although SU(3) symmetry is invoked, for obvious reasons, by both models to describe deformed nuclei, the physical and mathematical origins of this use as well as the specific SU(3) representations associated with the yrast bands are quite different in these two models.

If the PSM requires an upward normalization constant to obtain agreement with measured $B(E2)\uparrow$ values (as we contend it does with our choice of effective charges), so will the FDSM. We could quantify this renormalization in the case of the PSM, but not the FDSM, for the following reasons. In the FDSM the calculated quantities are the contributions of valence protons and neutrons to the reduced matrix elements (M_{π}^{ν} and M_{ν}^{ν}) of the quadrupole moment operator and *not* the intrinsic mass quadrupole moment. Equation (3) becomes

$$Q_0 = e_{\pi} M_{\pi}^{\nu} + e_{\nu} M_{\nu}^{\nu}. \quad (21)$$

Numerical values of M_{π}^{ν} and M_{ν}^{ν} (in units of b) have been provided by Wu [27], but they have been *already normalized* to fit the $B(E2)\uparrow$ value for ${}^{124}\text{Te}$ in the tin region, for ${}^{152}\text{Sm}$ in the rare-earth region, and for ${}^{226}\text{Ra}$ in the actinide region. The fit to an entire region can still be finetuned by rewriting Eq. (9) as

$$B(E2)\uparrow = (5/16\pi) C_{\text{FDSM}}^2 \times [(1 + ZA^{-1})M_{\pi}^{\nu} + (ZA^{-2}\epsilon)M_{\nu}^{\nu}]^2 e^2 b^2. \quad (22)$$

Wu [27] took $e_{\pi} = e_{\nu} = 1e$, whereas we prefer $e_{\pi} \approx 1.41e$ and $e_{\nu} = 0.82e$, corresponding to $\epsilon = 2.1$. With our ϵ value, Eq. (22), when applied to the data, yields C_{FDSM} values of 0.867 ± 0.009 , 0.856 ± 0.005 , and 0.985 ± 0.006 in the three regions [28], respectively (see Fig. 5). However, we cannot read much meaning into this C_{FDSM} as we did before with other models because the input quantities M_{π}^{ν} and M_{ν}^{ν} , calculated for the symmetry appropriate for each nucleus, are *not* absolute in the FDSM, nor are they related in any simple way to geometrical quadrupole moment because the FDSM effective quadrupole operator is quite different from the geometrical operator $r^2 Y_M^2$.

The $B(E2)\uparrow$ trends arise in the FDSM because of what has been called the “dynamic Pauli effect” specific to the structure (k - i decomposition of single-particle states) of its SU(3) symmetry for nucleons in normal-parity states. Such an effect is not contained in the PSM because, unlike the FDSM, it does not restrict these nucleons to S and D pairs. Nevertheless, Fig. 6 shows that good fits to $B(E2)\uparrow$ data in the actinide region are obtained with both the PSM and FDSM. In the rare-earth region (see Fig. 7), these two models invoke different groups, but

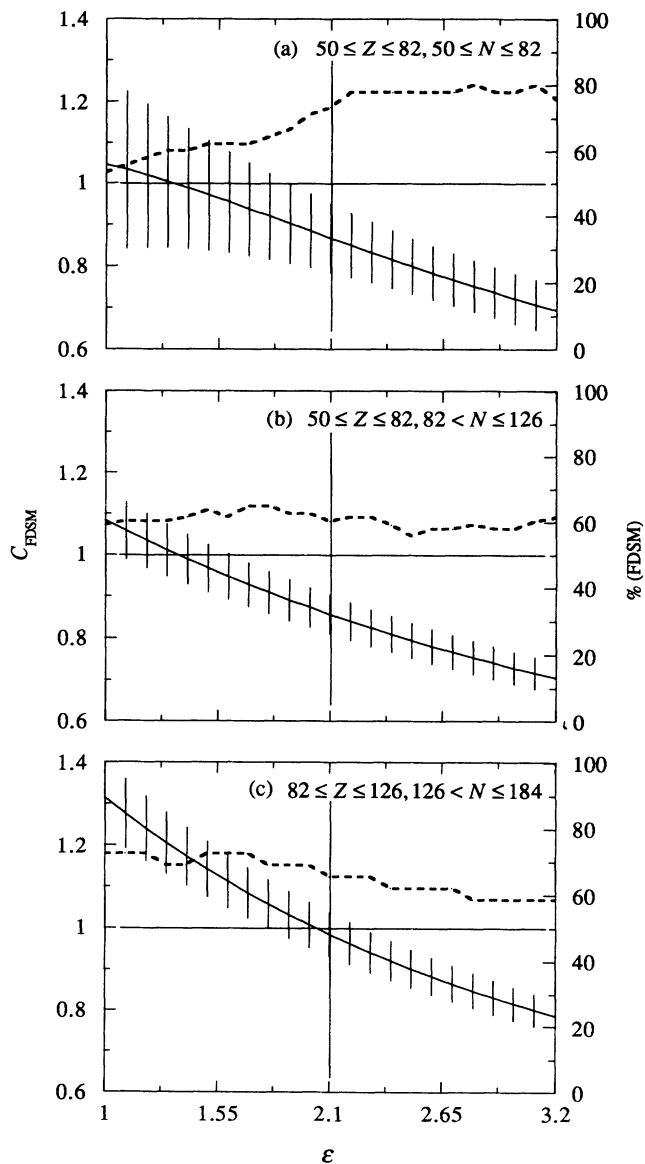


FIG. 5. Variation of the normalization constant C [see Eq. (22)] of the fermion dynamic symmetry model (FDSM) with the parameter ϵ . Solid curves (with error bars) give C (and its uncertainty) for the (a) tin region (45 nuclei), (b) rare-earth region (88 nuclei), and (c) actinide region (29 nuclei). Dashed curves denote the percentage of cases where calculated $B(E2)\uparrow$ values overlap within one standard deviation with measured values.

overall agreement with the data is good in both cases, thus implying that these $B(E2)\uparrow$ trends are not sensitive enough to the subtleties of the two models [29]. A similar insensitivity [30] was noted by us in Ref. [12], in which we presented the predictions of a variety of models and compared them with each other and with measurements.

VI. SUMMARY

If a nucleus is described in terms of a shell model, its intrinsic electric quadrupole moment depends on the mass quadrupole moments of the valence nucleons and their effective charges. We have argued that effective charges are usually meant to simulate only the core contribution to deformation (and hence to the $E2$ transition probability) and may not be used arbitrarily to compensate for the loss of quadrupole moments of valence nucleons due to restrictive assumptions of specific models

all within the same single-particle space. We have determined numerical values of “reasonable” effective charges. We have used them and our $B(E2)\uparrow$ compilation to calculate the fraction of the electric and mass quadrupole moments of deformed nuclei that is contributed by nucleons in abnormal-parity states. We concluded that in the single-shell asymptotic Nilsson model this fraction is typically $\sim 25\%$. The universal Woods-Saxon model also implies that nucleons in abnormal-parity states contribute about 20% to the electric quadrupole moment of a typical deformed nucleus.

Whether this amount can be considered negligible is, to some extent, a matter of choice influenced by necessity. The pseudo-SU(3) and fermion dynamic symmetry models make this choice by assuming that valence nucleons in (the high- j) abnormal-parity states remain in a state of seniority zero even in the presence of the polarizing effect of the maximally deformed state composed of the majority of nucleons which are in normal-parity states. Significant mathematical simplifications follow that

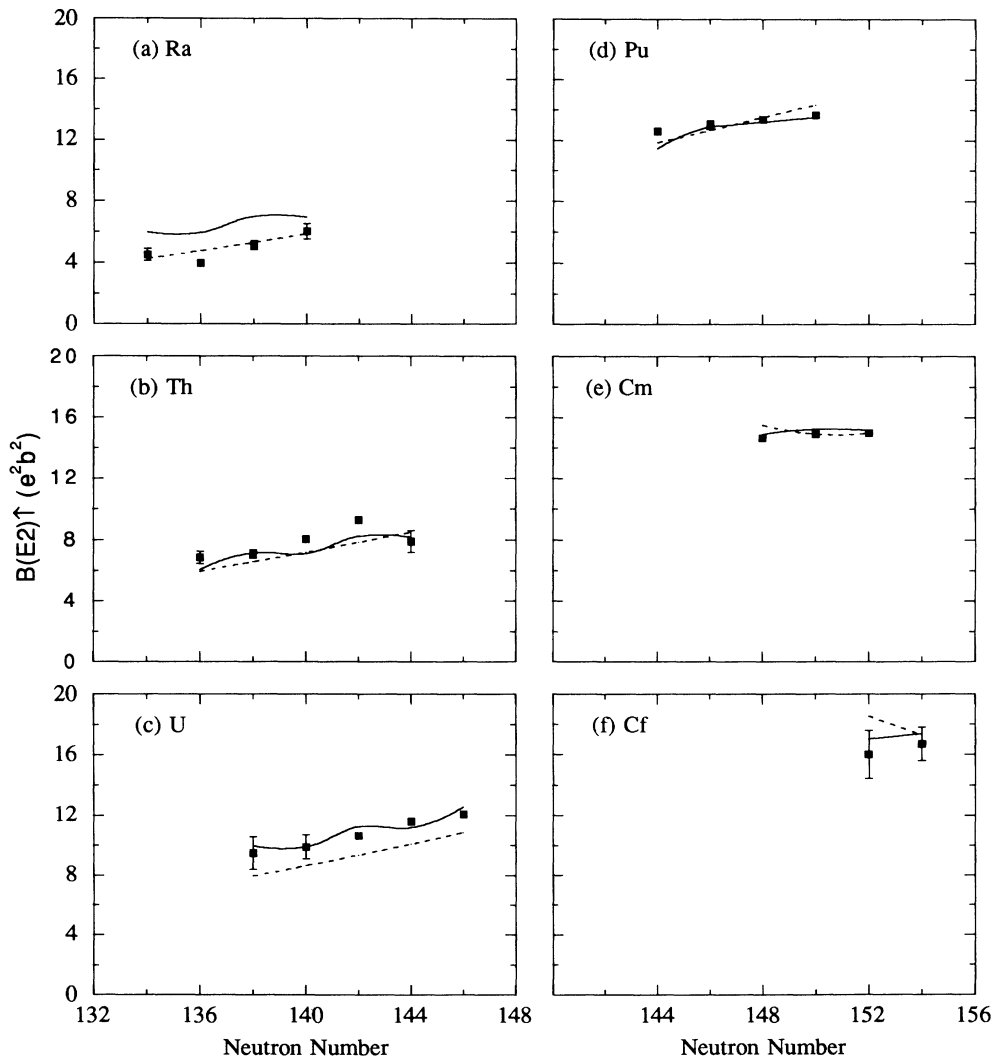


FIG. 6. Comparison between measured and calculated (with $\epsilon=2.1$) $B(E2)\uparrow$ values in the actinide region. Solid lines are the PSM predictions, dashed lines the FDSM.

enhance the practical utility of these models in terms of their predictive powers.

Our analyses show that this shunting of nucleons in the abnormal-parity states to a very minor role leads to a significant reduction of the intrinsic electric quadrupole moment in the pseudo-SU(3) model and, by inference, in the fermion dynamic symmetry model. Good agreement with measured $B(E2)\uparrow$ values consequently suffers, but can be restored by increasing the overall normalization constant. This success, in turn, may not be used to validate, advertently or otherwise, the basic assumptions of these models. In the case of $B(E2)\uparrow$ values, the normalization factors, which are often unstated or treated in a perfunctory fashion, contain interesting physics.

ACKNOWLEDGMENTS

We thank J. P. Draayer for explaining to us the intricacies of the pseudo-SU(3) model and for encouraging us to make the types of comparisons discussed in Ref. [12] with this model also. The FDSM matrix elements were kindly provided by Cheng-Li Wu. We acknowledge the help of Ramon Wyss in carrying out UWSM calculations. Witold Nazarewicz read the manuscript critically. One of us (K.H.B.) would like to thank J. Reidy, L. Riedinger, and J. B. Ball for facilitating his work at Oak Ridge. The current research was supported by the U.S. Department

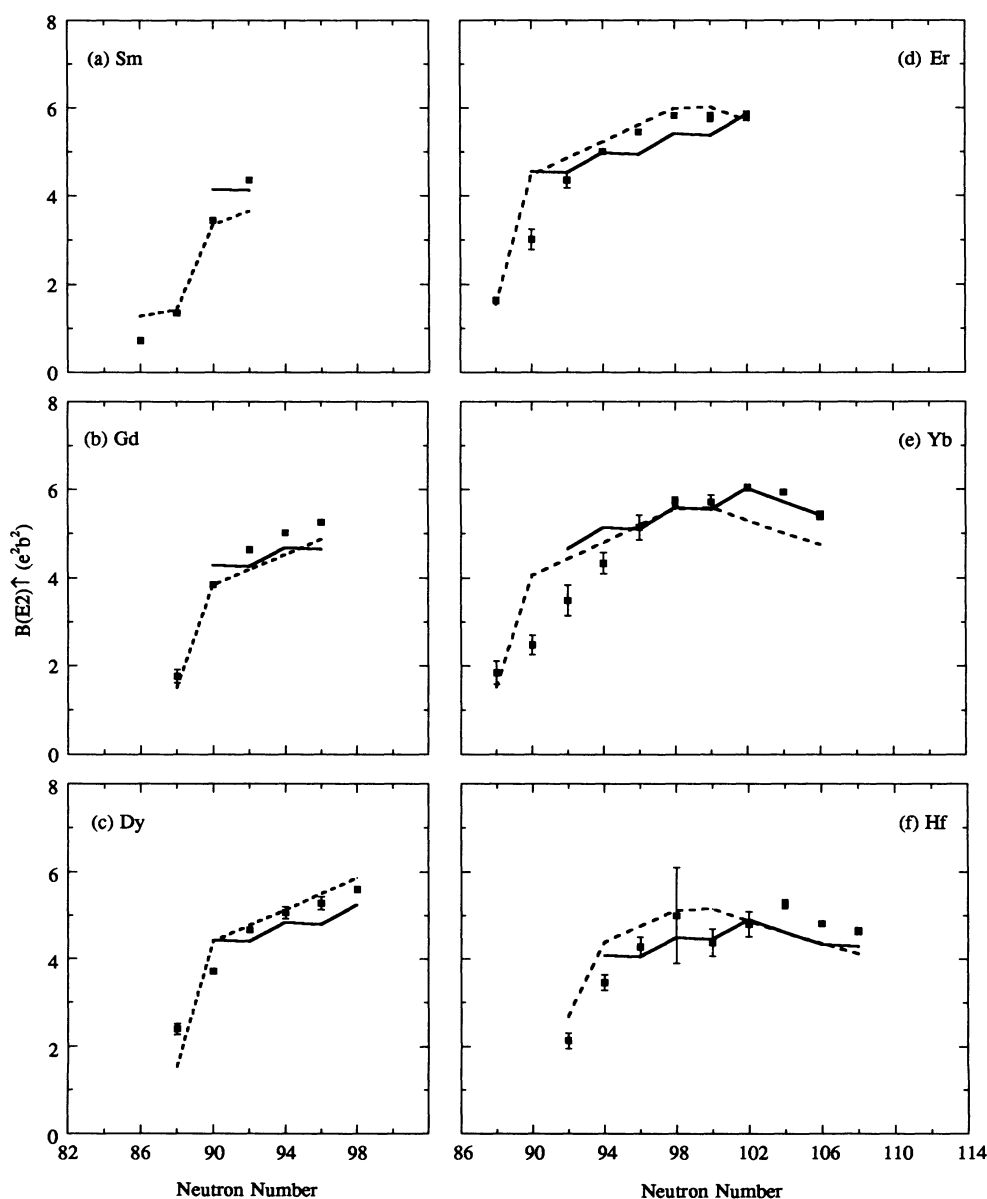


FIG. 7. Comparison between measured and calculated (with $\epsilon=2.1$) $B(E2)\uparrow$ values in the rare-earth region. Solid lines are the PSM predictions, dashed lines the FDSM.

of Energy under Contract No. DE-AC05-84OR21400 with Martin Marietta Energy Systems, Inc., for the operation of the Oak Ridge National Laboratory and Contract No. DE-AS05-76ERO-4936 with the Universi-

ty of Tennessee for the operation of the Joint Institute of Heavy Ion Research. The Joint Institute has as member institutions the University of Tennessee, Vanderbilt University, and the Oak Ridge National Laboratory.

-
- [1] S. Raman, C. H. Malarkey, W. T. Milner, C. W. Nestor, Jr., and P. H. Stelson, *At. Data Nucl. Data Tables* **36**, 1 (1987).
- [2] S. Raman, C. W. Nestor, Jr., S. Kahane, and K. H. Bhatt, *At. Data Nucl. Data Tables* **42**, 1 (1989).
- [3] P. Möller and J. R. Nix, *At. Data Nucl. Data Tables* **26**, 165 (1981).
- [4] S. Cwiok, J. Dudek, W. Nazarewicz, J. Skalski, and T. Werner, *Comput. Phys. Commun.* **46**, 379 (1987).
- [5] G. F. Bertsch, *The Practitioner's Shell Model* (North-Holland, Amsterdam, 1974), Chap. 7.
- [6] S. G. Nilsson, K. Dan. Vidensk. Selsk. Mat. Fys. Medd. **29**(16) (1955).
- [7] P. Ring and P. Schuck, *The Nuclear Many Body Problem* (Springer, New York, 1980).
- [8] W. Nazarewicz, in *Proceedings of the International Conference on Contemporary Topics in Nuclear Structure Physics*, Cocoyoc, México, 1988, edited by R. F. Casten, A. Frank, M. Moshinsky, and S. Pittel (World Scientific, Singapore, 1988), p. 467.
- [9] R. D. Ratna Raju, J. P. Draayer, and K. T. Hecht, *Nucl. Phys.* **A202**, 433 (1973). For more recent reviews of the PSM and its symplectic extensions, see J. P. Draayer, *ibid.* **A520**, 259c (1990) and in *Capture Gamma-Ray Spectroscopy*, Proceedings of the Seventh International Symposium on Capture Gamma-Ray Spectroscopy and Related Topics, edited by R. W. Hoff, AIP Conf. Proc. No. 238 (AIP, New York, 1991), p. 30.
- [10] C.-L. Wu, D. H. Feng, X.-G. Chen, J.-Q. Chen, and M. W. Guidry, *Phys. Lett.* **168B**, 313 (1986); *Phys. Rev. C* **36**, 1157 (1987).
- [11] S. Raman, C. W. Nestor, Jr., and K. H. Bhatt, *Phys. Rev. C* **37**, 805 (1988).
- [12] S. Raman, C. W. Nestor, Jr., S. Kahane, and K. H. Bhatt, *Phys. Rev. C* **43**, 556 (1991).
- [13] S. Kahane, S. Raman, and J. Dudek, *Phys. Rev. C* **40**, 2282 (1989).
- [14] F. Villars, in *Many-Body Description of Nuclear Structure and Reactions*, Proceedings of the International School of Physics "Enrico Fermi," Course XXXVI, Varenna on Lake Como, 1965, edited by C. Bloch (Academic, New York, 1966), p. 31.
- [15] A. Bohr and B. R. Mottelson, *Nuclear Structure* (Benjamin, Reading, MA, 1975), Vol. II, p. 523.
- [16] A. P. Byrne, R. Müseler, H. Hübel, K. H. Maier, and K. Kluge, *Nucl. Phys.* **A516**, 145 (1990).
- [17] E. K. Warburton and B. A. Brown, *Phys. Rev. C* **43**, 602 (1991).
- [18] S. Yoshida and L. Zamick, *Annu. Rev. Nucl. Sci.* **22**, 212 (1972).
- [19] R. C. Thompson, M. Anselment, K. Bekk, S. Göring, A. Hanser, G. Meisel, H. Rebel, G. Schatz, and B. A. Brown, *J. Phys. G* **9**, 443 (1983).
- [20] S. Raman and J. B. McGrory, Oak Ridge National Laboratory Annual Progress Report No. ORNL-6578, 1989, p. 194.
- [21] In the rare-earth and actinide regions, the ZA^{-1} factors vary little for those nuclei with measured $B(E2)\uparrow$ values—they are in the 0.38–0.46 and 0.38–0.41 ranges, respectively, with median values of 0.412 and 0.395. Hence we recommend $e_\pi=1.41e$ and $e_\nu=0.82e$ corresponding to $\epsilon=2.1$ in Eq. (5) for general use in these two regions.
- [22] J. P. Elliott, *Proc. R. Soc. London A* **245**, 128 (1958); **245**, 562 (1958).
- [23] M. Harvey, in *Advances in Nuclear Physics*, edited by M. Baranger and E. Vogt (Plenum, New York, 1968), Vol. 1, p. 67.
- [24] We infer from Table VIII that the PSM predicts triaxial intrinsic states for most nuclei including ^{154}Gd .
- [25] O. Castaños, P. O. Hess, J. P. Draayer, and P. Rochford, *Nucl. Phys.* **A524**, 469 (1991).
- [26] O. Castaños, J. P. Draayer, and Y. Leschber, *Ann. Phys. (N.Y.)* **180**, 290 (1987).
- [27] C.-L. Wu (private communication).
- [28] In Ref. [12] we obtained much higher C_{FDSM} values of 22.3 (rare earths) and 17.3 (actinides) because we had incorrectly assumed that the matrix elements supplied by Wu [27] were in units of α^2 , whereas they actually were in units of b.
- [29] It will be difficult in practice to use the PSM SU(3) basis to describe collective states of spherical and transitional nuclei, whereas the FDSM, like the interacting boson approximation (IBA) before, provides a fairly good description of these states even in the limit of exact symmetry appropriate for such nuclei.
- [30] This insensitivity will quickly disappear if the normalization constant and effective charges are optimized for one model and carried over to another. See, for instance, D. H. Feng, C.-L. Wu, M. W. Guidry, and Z.-P. Li, *Phys. Lett. B* **205**, 156 (1988). If the normalization constants appropriate to the FDSM are also adopted for the IBA, as these authors have done, the agreement is poor between measured $B(E2)\uparrow$ values and IBA predictions.